Lipid-Induced Conformational Transitions of β-Lactoglobulin†

Xiuqi Zhang and Timothy A. Keiderling*

Department of Chemistry, University of Illinois, 845 West Taylor Street (m/c 111), Chicago, Illinois 60607-7061

Received February 10, 2006; Revised Manuscript Received May 5, 2006

ABSTRACT: Bovine β-lactoglobulin (βLG) provides an excellent model protein system for β-to-α conformational change, but its behavior varies when the change is induced by alcohols, surfactants, or lipid vesicles. Here the interaction and orientation of βLG in association with various artificial lipid vesicles at neutral and acidic pH have been studied by use of several complementary spectroscopic techniques. Circular dichroism (CD) and Fourier transform infrared (FTIR) spectra demonstrated that βLG acquires a non-native α-helical structure upon binding with anionic lipids, while zwitterionic lipids do not have a significant effect on its conformation. The degree of induced α-helix depends on the lipid concentration and is strongly affected by the charge of the protein and lipids as well as the ionic strength of the solution. Near-UV CD and Trp emission spectra revealed that the tertiary structure of lipid-bound βLG is highly expanded but not completely disrupted. Fluorescence quenching together with a Trp emission blue shift showed that the Trp residues remain largely shielded from the solvent when interacting with DMPG, which would be consistent with at least some portions of βLG having been inserted into the lipid membrane. The orientations of the α-helix and β-sheet axes in membrane-bound βLG were found to be parallel and perpendicular, respectively, to the membrane film normal, as determined by use of polarized attenuated total reflection (ATR) FTIR spectra. Our findings reveal that the lipid-induced β-to-α transition in βLG, accompanied by a substantial disruption in tertiary structure, is mainly driven by strong electrostatic interactions. Once the tightly packed βLG is disrupted, hydrophobic residues become exposed and available for insertion into the lipid bilayer, where hydrophobic interaction with the lipids may play a role in stabilizing the helical components.

Bovine β-lactoglobulin (βLG)[1] is a member of the family of so-called lipocalins or lipocalycins, which are widely valued by the food industry for emulsifying and emulsion-stabilizing properties (*1*). βLG is a globular protein with a monomer molecular weight of approximately 18 300 and exists in various oligomeric states as a function of pH, temperature, concentration, and genetic variant. In the native state, βLG has a predominantly β-structure, consisting of one α-helix and nine antiparallel β-strands, forming a flattened β-barrel core (*2*), which provides a binding site for a wide variety of amphiphilic or hydrophobic ligands, including surfactants, fatty acids, many small alkanes, aliphatic ketones, and a number of simple and complex ions (as reviewed in ref *1*). This binding ability has been related to a possible physical function of βLG as a carrier of retinal and fatty acids, thereby preventing inhibition of preduodenal lipases and facilitating the digestion of milk fat (*3*).

Intriguingly, secondary structure algorithms predict a significant propensity for some β-strand segments, particularly the three N-terminal strands, in the βLG sequence to form helices (*4*). Non-native helical structure was observed during an early stage of βLG folding (*5*, *6*). On the basis of similar observations, the nonhierarchical folding hypothesis has been suggested for the folding of βLG (*7*, *8*). Therefore, βLG is an excellent model protein for studying internal structural rearrangement pathways as opposed to direct folding pathways from the denatured state. The nature of these transitions and the stability of any α-helical intermediates are dependent on the mechanism for inducing them, as we will demonstrate. Finally, βLG is a good model for understanding the conversion from short-range interactions between nearby amino acid residues stabilizing the α-helical structure and long-range interactions between secondary structures stabilizing the β-sheet structure.

Consistent with its high helical propensity, βLG is known to exhibit a high level of non-native helical structure in the presence of alcohols (*9*), ionic surfactants (*10*), and lipids (*11*). It has been recognized that alcohol-induced α-helical formation follows two processes: disruption of the native state as a result of weakening of nonlocal interaction through hydrophobic interaction between micellelike assembled alcohols and the native state and induction of an α-helical conformation as a result of enhancement of the local hydrogen bonds (*12*). Nevertheless, the TFE-induced non-native α-helical structure is unstable and converts readily to

† This work was supported in part for equipment purchases by grants from the Research Corp., the National Science Foundation (CHE00-0316014), and a fellowship (to T.A.K.) from the John Simon Guggenheim Foundation.

* To whom correspondence should be addressed. E-mail: tak@uic.edu. Fax: (312) 996-0431. Phone: (312) 996-3156.

[1] Abbreviations: DMPG, dimyristoylphosphatidylglycerol; DMPC, dimyristoylphosphatidylcholine; SUVs, small unilamellar vesicles; MLV, multilamellar liposome suspension; LUVs, large unilamellar vesicles; βLG, β-lactoglobulin; CD, circular dichroism; FTIR, Fourier transform infrared; ATR-FTIR, attenuated total reflection Fourier transform infrared.

10.1021/bi0602967 CCC: $33.50
Published on Web 06/15/2006

an intermolecular antiparallel β-sheet aggregate through a gradual and time-dependent process (*13*). Likewise, ionic surfactants also can induce non-native α-helical structure in βLG; however, such non-native α-helical structure is more stable toward thermal and chemical denaturation than the native state (*10*). It has been suggested that surfactants may cause a reduction in the extent of hydrogen bonding between the protein molecule and the solvent water due to the shielding of hydrogen bonding entities of the protein by the bound surfactant molecules. Then the protein molecule tends to form intramolecular hydrogen bonds, thereby promoting the formation of α-helices (*14*).

Phospholipids, in general, are important constituents of biological systems in which the phospholipid bilayer forms the basic element of the cell membrane. They are commonly found in foods. For example, milk fat globule membrane consists of 27% (w/w) phospholipids (*1*). Because it is one of the major milk proteins, interaction of βLG with phospholipids is therefore of great importance. Some studies on the interaction between βLG and phospholipids at the air−water interface have been reported (*15*−*17*). It was postulated that the mechanism for the interaction of βLG with a phospholipid monolayer consisted of a three-step process. First, the βLG adsorbs onto the membrane surface; second, the protein binds to the phospholipids, and finally, some parts of the protein insert into the monolayer (*16*). The interaction between βLG and phospholipids at a liquid interface was found to depend on both the headgroup and the hydrophobic chain of the phospholipid (*17*). The interaction of βLG with phospholipids in the gel and liquid-crystalline phases has been studied by using infrared spectroscopy (*11*, *18*). Mutual interactions were found between anionic membrane and βLG; however, zwitterionic lipids had little effect on the conformation of βLG, and in turn, they are less affected by βLG.

Despite previous work carried out on this protein, the role of hydrophobic and electrostatic interactions in binding of βLG with membranes remains unclear. In particular, the evolution of secondary and tertiary structure, the structure of lipid-bound βLG, the structural requirements for βLG penetrating into lipid membrane, and the preferable orientation of βLG within the lipid membrane are still poorly understood. In this study, complementary equilibrium spectroscopies were used to address these questions by using one type of artificial lipid with different headgroups to form model membranes. Circular dichroism (CD) and Fourier transform infrared (FTIR) spectra together with Trp fluorescence were used to determine the dependence of secondary and tertiary structure on the protein−lipid interactions, as well as other perturbations, while fluorescence quenching and polarized attenuated total reflection (ATR) FTIR were used to demonstrate incorporation of βLG into and its orientation within the membrane. Different non-native α-helical states induced by alcohols, surfactants, and lipids are compared in the analysis of our results.

MATERIALS AND METHODS

Materials. Bovine βLG, crystallized and lyophilized three times, was purchased from Sigma (catalog no. L 3908, St. Louis, MO) and used without further purification. Dimyristoylphosphatidylglycerol (DMPG) and dimyristoylphosphatidycholine (DMPC) were obtained from Avanti Polar Lipids, Inc. (Alabaster, AL). Organic solvents (methanol and chloroform, spectral-grade) and sodium phosphate (analytical-grade) were purchased from Sigma, and deuterium oxide was purchased from Cambridge Isotope Laboratories, Inc.

Preparation of Lipid Vesicles. Fresh small unilamellar vesicles (SUVs) were prepared by sonication using literature techniques just before being used (*19*). The required amount of dried lipid was then dispersed in the desired buffer (10 mM phosphate buffer for pH 6.8 or 4.6) and then vortexed extensively. The resulting multilamellar liposome suspension (MLV) was then immersed in a bath sonicator (Branson 2200, Bransonic) until the MLVs were dispersed into a clear suspension of SUVs, typically after ∼30−90 min. The temperature of the bath sonicator was kept less than ∼10 °C above the lipid transition temperature via exchange of cool water. For binary lipid mixtures, the lipids were dissolved in a chloroform/methanol mixture (3:1, v/v) for various ratios of DMPC to DMPG, and the resulting lipid solutions were dried under a mild stream of N_2 while being shaken gently to form a thin film on the vial wall. The film was then hydrated by adding the desired buffer. The hydrated suspension was vortexed, frozen and thawed, and then dispersed by use of a bath sonicator until the solution was clear to form SUVs. βLG was incorporated into the vesicles by slowly adding it to the aqueous lipid vesicle solution, and then the resulting solution was mixed well. Binding of βLG and vesicles was allowed to equilibrate for 1 h prior to the study of the protein−lipid complexes that formed. For IR measurements, large unilamellar vesicles (LUVs) prepared by extrusion were used. Efforts to determine vesicle size by means of dynamic light scattering and TEM were inconclusive but suggested the resultant vesicles were larger than expected for SUVs, presumably due to formation of a lipid membrane network caused by melting in the temperature range used for dynamic light scattering measurements (*20*).

Circular Dichroism. CD spectra were measured on a J-810 spectrometer (Jasco, Easton, MD) using quartz cells with path lengths of 1 mm and 1 cm for protein concentrations of 0.2 and 2 mg/mL, respectively, in the far- and near-UV CD. Typically, a scanning rate of 50 nm/min and a bandwidth of 0.5 nm with a time response of 2 s were used to obtain CD spectra as an average of four scans. The final spectra were obtained by subtracting a background spectrum obtained on just buffer or vesicles without protein in the same cell. The fractional secondary structure of the samples was estimated from the CD spectra by use of the SELCON 3 method, which is part of the CDPro software package (*21*). Scattering could be a problem with CD measurements on lipid vesicle samples (*22*), but our results for DMPC and βLG measured over a wide concentration range that show quantitative agreement with the βLG CD spectrum suggest that light scattering is not a problem for the SUVs used in this work.

Oriented CD measurements were performed following methods described previously (*23*, *24*). Oriented CD spectra were recorded every 22.5° of rotation of the sample holder, and then the 16 resulting spectra were averaged.

FTIR and ATR-FTIR Measurements. FTIR measurements were performed as previously described (*25*, *26*). Briefly, βLG was dissolved in 10 mM deuterated PBS buffer to a final concentration of 3 mg/mL in the absence and presence of 27 mM DMPG LUVs. Then the samples were transferred

to a homemade demountable cell composed of two CaF_2 windows separated by a 100 μm Teflon spacer clamped together in a brass holder. The FTIR spectra were recorded at a nominal resolution of 4 cm^{-1} by averaging 512 scans obtained on a FTS60A spectrometer (Digilab, Randolph, MA).

ATR-FTIR experiments were carried out on a FTS60A spectrometer using a MIRacle ATR accessory (PIKE Technologies, Inc., Madison, WI), equipped with a three-reflection ZnSe ATR Universal Plate. Approximately 10 μL of a βLG/DMPG mixture was pipetted onto the recessed ZnSe plate and then dried under a gentle stream of nitrogen gas to form a thin film on the surface. To obtain polarized ATR spectra, a wire grid polarizer was placed in front of the sample and spectra were recorded for 0° and 90° polarizations of the incident light beam. The dichroic spectra were obtained by subtracting a spectrum recorded with light polarized in a parallel fashion from that recorded with light polarized in a perpendicular fashion, using a weight coefficient, R_{iso}, defined as the ratio of integrated absorbance of the lipid carbonyl band in spectra measured with parallel polarization of the incident light to the absorbance measured with perpendicular polarization of the incident light (*27*, *28*).

Fluorescence Measurements. Fluorescence measurements were performed on a Fluoromax-3 spectrofluorometer (Jobin Yvon Inc., Edison, NJ). The excitation wavelength was 295 nm, and the emission was scanned from 300 to 450 nm. In all experiments, background spectra, either the buffer alone or the buffer containing vesicles, were subtracted from the corresponding sample spectra. The concentration of βLG for all fluorescence measurements was kept at ~0.2 mg/mL. For fluorescence quenching experiments, small aliquots of a 5 M acrylamide stock solution were added to the βLG in the absence or presence of lipid vesicles, and the fluorescence emission spectra were recorded at an excitation wavelength of 295 nm to reduce contributions from the absorbance of acrylamide ($\lambda_{max} \sim 280$ nm). The data were analyzed according to the Stern−Volmer equation, $F_0/F = 1 + k_{sv}[Q]$, where F_0 and F are the fluorescence intensities in the absence and presence of the quencher, respectively, while k_{sv} is the Stern−Volmer quenching constant, which is a measure of the accessibility of acrylamide to Trp residues (*29*).

RESULTS

Lipid-Induced Conformational Change of βLG. CD, FTIR, and fluorescence were used to probe secondary and tertiary structural changes in βLG upon interaction with lipids. As shown in Figure 1A (dotted line), the far-UV CD spectrum of βLG in aqueous solution at neutral pH exhibits a wide minimum around 216 nm, a feature typical of β-sheet-dominant proteins. With the addition of anionic DMPG vesicles, however, CD spectra of βLG change in a manner characteristic of a transition from β-sheet to α-helix (Figure 1A, solid lines), developing two minima at ~208 and ~222 nm. The inset in Figure 1A traces the change in ellipticity at 222 nm as a function of DMPG concentration. At neutral pH, the ellipticity at 222 nm increased linearly with the increase in the DMPG concentration to 0.4 mM, and thereafter, it reached a plateau (saturated) relatively independent of any further increase in the concentration of DMPG. The estimated secondary structure changes [determined using SELCON 3 (*21*)] as a function of DMPG concentration are presented in Figure 1B. It was found that the content of DMPG-induced α-helix at neutral pH reached a plateau (~36%) when the DMPG concentration was >0.5 mM. Moreover, an increase in the α-helix fraction was correlated with a decrease in β-sheet content; i.e., the formation of α-helix was at the expense of β-sheet, clearly indicating a transition from native β-structure to lipid-bound non-native α-helical structure. At the low concentration of DMPG, the β-to-α transition is highly cooperative.

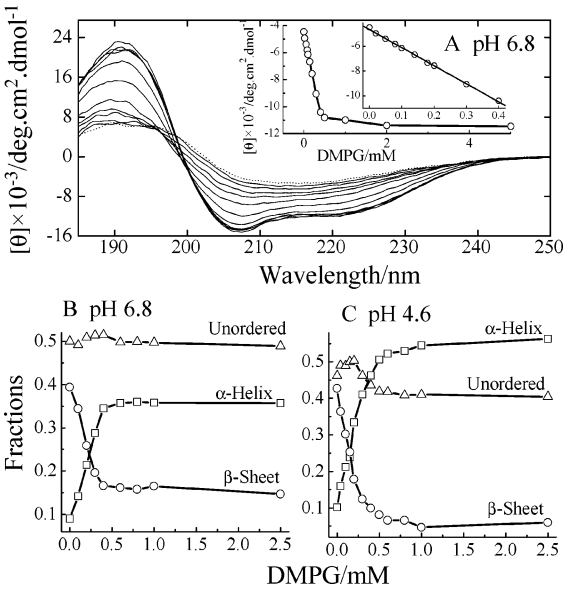

FIGURE 1: DMPG-dependent conformational transition of βLG measured by far-UV CD (mean molar ellipticity per residue). (A) Representative far-UV CD spectra of 0.2 mg/mL βLG in the absence (···) and presence of various concentrations of DMPG at pH 6.8 (—). The inset shows the change in the ellipticity at 222 nm as a function of DMPG concentration. (B and C) Estimated fractional secondary structures as a function of lipid concentration at pH 6.8 and 4.6, respectively.

Likewise, at pH 4.6, DMPG can also induce the formation of non-native α-helix in βLG. As depicted in Figure 1C, when the concentration of DMPG is below 0.25 mM, the content of α-helix increased proportionally with an increase in DMPG concentration, and the α-helix forms at the cost of β-sheet. With the further increase in the concentration of DMPG, however, the α-helix increase depletes unordered structures, which is in contrast to the results at pH 6.8 (Figure 1B). Compared with the DMPG-induced α-helix (~36%) at pH 6.8, more α-helix (~53%) was induced at pH 4.6, indicating a stronger βLG−DMPG interaction resulting in a full change of the βLG conformation. When the DMPG concentration is close to 0.5 mM, at pH 4.6, the secondary structure content reached a plateau at >53% α-helix but ≤5% β-sheet, values that must be considered approximate only, since these more extreme secondary structure ranges are often difficult to predict accurately for globular proteins (*30*). At higher βLG concentrations, this α-to-β transition occurs at a higher DMPG concentration (see below).

As an independent control, FTIR spectroscopy was used to confirm the lipid-induced conformational changes of βLG. Figure 2 shows FTIR spectra (bottom panel) and inverted second-derivative spectra (top panel) of 3 mg/mL βLG in a 10 mM PBS/D_2O solution (dotted line) and in a 27 mM DMPG/D_2O solution (solid line). The major peaks in the

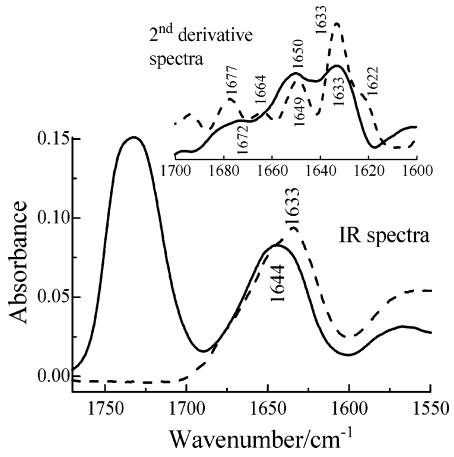

FIGURE 2: FTIR (bottom panel) and inverse second-derivative spectra (top panel) of 3.0 mg/mL βLG in deuterated PBS (pH 6.8, - - -) and in the presence of a 27 mM DMPG/D_2O solution (pH 6.8, —).

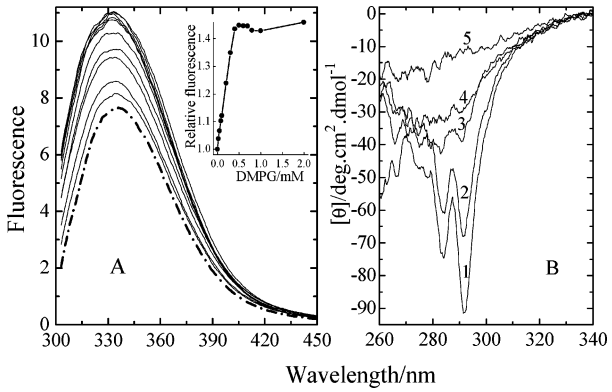

FIGURE 3: DMPG-dependent tertiary structure change measured by (A) fluorescence of 0.2 mg/mL βLG (λ_{exc} = 295 nm) in the absence (—•—) and presence of various concentrations of lipid at pH 6.8 (—). The inset shows the normalized fluorescence intensity at λ_{max} as a function of lipid concentration. (B) Near-UV CD spectra of 1.3 mg/mL βLG in the presence of 0 (curve 1), 1.0 (curve 2), 2.5 (curve 3), and 9.0 mM DMPG (curve 4) and 6 M GdnHCl (curve 5) at pH 6.8.

second-derivative FTIR spectra (plotted to be positive), at 1633 and 1622 cm^{-1} in the spectrum of βLG in PBS buffer (pH 6.8), are assigned to β-sheets, whereas the one at 1650 cm^{-1} is related to α-helix and unordered structures (*18*). By contrast, the second-derivative FTIR spectrum of DMPG-bound βLG is composed of three broad components, located at 1632, 1650, and 1673 cm^{-1}. A clear transition from β-structure (features at 1634 and 1622 cm^{-1}) to α-structure (relative growth at 1650 cm^{-1}) is induced by binding of βLG to DMPG vesicles as evidenced by changes in the relative intensity and bandwidth for each component, consistent with the β-to-α transition observed above with far-UV CD spectra.

Lipid-induced changes in βLG secondary structure are accompanied by tertiary structural changes evidenced as a decrease in the near-UV CD intensity (Figure 3B). The spectrum of native protein in buffer (pH 6.8, trace 1) shows two sharp negative bands centered at ∼292 and ∼284 nm that can be ascribed to tryptophan vibrational fine structure, while the two bands located at ∼277 and ∼265 nm depend mainly on tyrosines (*31*). With an increasing DMPG concentration (traces 2−4), the structured peaks of the near-UV CD at ∼292 and ∼284 nm (Trps) and ∼277 and ∼265 nm (Tyrs) collapse to a broad negative band between 2.5 and 9 mM DMPG. However, even in the presence of 9 mM DMPG, the magnitude of the CD signal is greater than that of βLG in 6 M GdnHCl (trace 5). While this may indicate restricted motion, the lack of definition in the spectra is consistent with the overall loss of tertiary structure. The near-UV CD may have a contribution from the disulfide bonds as well, which normally give rise to broad weak signals throughout the near-UV spectra (*32*). The apparent higher stability of the Trp−Trp interaction as seen in near-UV CD is an effect of concentration. If the far-UV CD (helix content) dependence on DMPG were measured at this higher βLG concentration, a higher DMPG concentration would be required for β-to-α conversion. However, if the ellipticity changes were plotted versus the lipid:protein ratio, the traces at both βLG concentrations would reach the maximum at virtually the same lipid:protein ratio (data not shown). These results indicate that the change from a dominant β- to α-secondary structure is correlated with tertiary structural loss, which must have important mechanistic consequences for unfolding.

As an alternate probe of tertiary structure change, fluorescence spectra of βLG in various concentrations of DMPG vesicles were measured (Figure 3A). In the absence of DMPG (dashed line), the fluorescence maximum (λ_{max}) was ∼336 nm, indicating the emitting tryptophan residues might be in a shielded hydrophobic environment. With the addition of DMPG (solid lines), the fluorescence intensities increased, suggestive of a decreased level of quenching due to increased motional flexibility for Trp61, which in the native state is highly quenched by a nearby disulfide group (*33*). Meanwhile, there is a small blue shift (∼4 nm), suggesting that Trp19 and/or Trp61 becomes increasingly shielded to some extent by insertion into the lipid membrane. As shown in the inset of Figure 3A, the normalized fluorescence intensity reached a maximum at ∼0.5 mM DMPG, in good agreement with the far-UV CD data (obtained for the same samples), again suggesting the tertiary structural changes are correlated to the secondary structural changes.

In contrast to DMPG, zwitterionic phospholipids (DMPC) alone induce neither non-native α-helix nor significant tertiary structure (data not shown) in the test concentration range. These results indicate that zwitterionic lipids alone have much weaker interaction with βLG, insufficient to induce a significant perturbation in the βLG conformation. The far-UV spectra of these samples were virtually constant with an increase in DMPC concentration from 0 to 2 mM, additionally confirming that our experimental results are relatively free of scattering artifacts.

Driving Force for Binding of βLG to DMPG Membranes. To investigate the role that electrostatic interactions play in the association of βLG with lipids, some governing variables, such as protein charge, lipid charge, and ionic strength, have been examined through their impact on βLG far-UV CD measurements.

The net charge can be manipulated by changing the pH to protonate or deprotonate the proteins in solution. βLG has a net charge of approximately −8 at pH 6.8, and between 8 and 10 at pH ∼4.4, with an isoelectric point of 5.5 (*34*). Figure 4A depicts the changes in secondary structural fractions of DMPG-bound βLG as a function of pH. Clearly, a lower pH favors the formation of non-native α-helix, indicating that electrostatic interaction between lipid vesicles

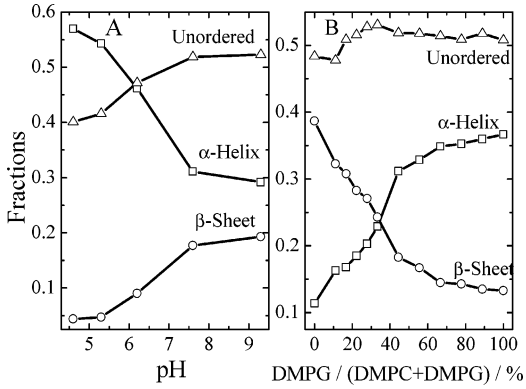

FIGURE 4: Charge-dependent secondary structural fractions measured by far-UV CD via changing pH (A) and lipid charge (B). βLG (0.2 mg/mL) in the presence of 1.0 mM DMPG (A) and a 1.8 mM DMPG/DMPC mixture with varying DMPG:DMPC ratios (B), estimated by SELCON 3 of CDPro.

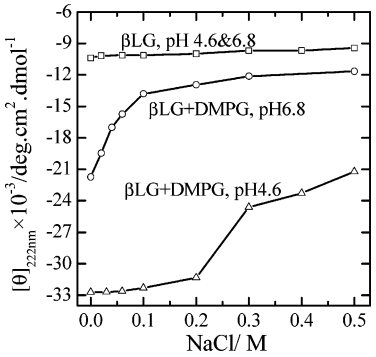

FIGURE 5: Effect of ionic strength on the binding of βLG to DMPG followed by far-UV CD: 0.2 mg/mL βLG in 10 mM PBS (□) and 0.2 mg/mL βLG in 1.0 mM DMPG at pH 6.8 (○) and 4.6 (△).

and proteins plays a key role in the lipid-induced formation of non-native α-helix. At pH values above its isoelectric point, βLG can still bind to anionic DMPG, which in turn disturbs its conformational structure. However, the magnitude of the perturbation is decreased as compared to that evidenced at low pH, suggesting that the interaction of βLG with lipid is highly dependent on pH and consequently on the net charge of the protein.

To further confirm the importance of electrostatic forces in the interaction between βLG and lipid membranes, the net mean charge of the lipid vesicles was varied by adjusting the ratio of DMPG to DMPC in the lipid mixture while maintaining a fixed total lipid concentration. This approach keeps a constant hydrophobic component but varies the charge. The fractional changes in βLG secondary structures with an increasing proportion of DMPG are summarized in Figure 4B, showing the content of α-helix increases with an increasing lipid charge (increased DMPG concentration). The existence of DMPC in the mixture cannot facilitate a further increase in the α-helix content, implying that, whereas the electrostatic interaction plays a key role in the interaction between βLG and DMPG vesicles, hydrophobic interactions must have a minor role.

The effect of ionic strength was examined in further investigating the role of electrostatic interactions. Generally, if electrostatic interactions are important for the binding, increased ionic strength would weaken the binding of βLG to the negatively charged membrane surface. Figure 5 shows the changes in ellipticity at 222 nm, characteristic of helix,

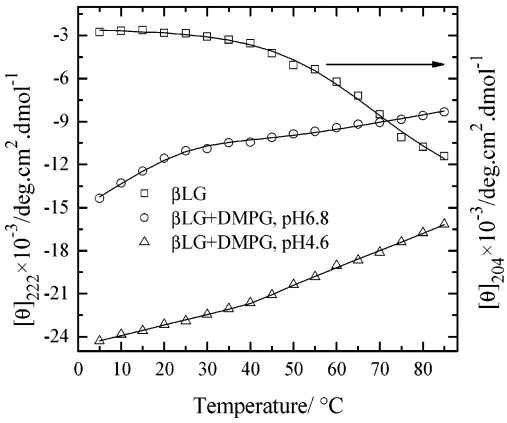

FIGURE 6: Thermal stability followed by the ellipiticity of far-UV CD at 204 and 222 nm for 0.26 mg/mL βLG alone (□) and 0.26 mg/mL βLG in the presence of 1 mM DMPG at pH 4.6 (△) and 6.8 (○).

for βLG in the absence and presence of lipids as a function of an increasing NaCl concentration at pH 6.8 and 4.6. At both pHs, the increasing NaCl concentration has a negligible effect on the pure βLG (□). However, for 0.2 mg/mL βLG in 1.0 mM DMPG at pH 6.8 (○), the addition of NaCl (>0.1 M) sharply decreased the helical content (monitored by $[\theta]_{222}$), and thereafter, it reached a plateau. At pH 4.6, by contrast, addition of NaCl (<0.2 M) had a negligible effect on the lipid-induced helix, indicating that the DMPG−βLG complex is relatively stable at lower pH (△). High concentrations of NaCl (>0.2 M) did result in a decrease in ellipticity. These data suggest that the addition of NaCl largely dissociates βLG from the negatively charged lipid at neutral pH, while at acidic pH, higher concentrations of NaCl are required and the dissociation is less complete. Thus, the interaction with lipid is not complete with only charge neutralization, but it provides a mechanism of attaining access to the hydrophobic core of the bilayer. It is interesting to note that at both pHs, the addition of more NaCl (up to 0.5 M) did not completely dissociate βLG from DMPG, which is consistent with at least a portion of the βLG being inserted into the bilayer.

Thermal Stability of the Lipid−βLG Complex. Figure 6 compares the thermal stability of the lipid-bound βLG complex to that of βLG alone at pH 6.8 and 4.6, studied by the change in the far-UV CD spectra. With an increase in temperature, βLG underwent β-to-coil transition with a T_m of ~68 °C, as monitored by the ellipticity at 204 nm (□). By contrast, for a βLG−DMPG complex at both pH 6.8 (○) and 4.6 (△), the ellipticity at 222 nm decreases with an increase in temperature without showing a clear transition. However, the βLG−DMPG complex conserves a high degree of helical structure (28 and 46% for pH 6.8 and 4.6, respectively) even at 85 °C as compared to the native protein. The decrease in the level of helical structure caused by temperature may be due to dissociation of the DMPG-bound βLG or due to unfolding of the βLG−DMPG complex. The temperature-dependent intrinsic fluorescence intensity shows quite similar traces with decreasing intensity for both βLG and the βLG−DMPG complex, while the λ_{max} of βLG and the βLG−DMPG complex changes quite differently. Whereas λ_{max} shows a significant change for the native βLG, there is no significant change in λ_{max} for the βLG−DMPG complex at both pHs when the temperature is above 60 °C (data not

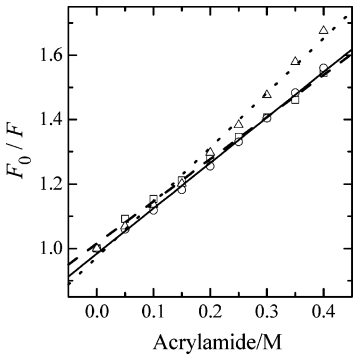

FIGURE 7: Stern−Volmer plots for acrylamide quenching of Trp fluorescence for 0.2 mg/mL βLG in the absence (□) and presence of 2.5 mM DMPG at pH 4.6 (○) and 6.8 (△).

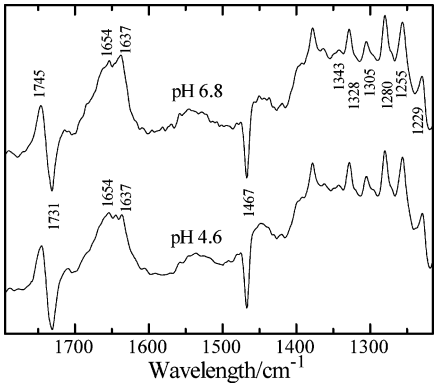

FIGURE 8: Polarized ATR-FTIR difference spectra (90°−0° polarization) of DMPG-bound βLG (250:1 DMPG:βLG molar ratio) at pH 4.6 (bottom trace) and 6.8 (top trace). For clarity, the spectra were offset.

shown). This result suggests that the decrease in the level of helical structure caused by varying temperature is mainly due to the unfolding of βLG rather than the dissociation of the βLG−DMPG complex. The level of recovery of the βLG−DMPG complex is 95 and 83% for pH 6.8 and 4.6, respectively, suggesting that the insertion may increase the possibility of the complex unfolding with an irreversible component under thermal perturbation.

Binding and Insertion of βLG into Lipid Vesicles. Fluorescence quenching is often used to assess the shielding of tryptophan residues from the solvent as proteins fold or insert into lipid membranes (*29*). Figure 7 shows Stern−Volmer plots of the quenching of the Trp fluorescence in βLG by acrylamide, recorded in the absence and presence of DMPG vesicles at different pHs. Increasing the concentration of quencher resulted in a decrease in the fluorescence intensity in both media. However, this effect is almost the same in the presence of vesicles at pH 4.6 and 6.8 as in buffer alone, indicating that the accessibility of the fluorophore did not change substantially through βLG expansion as induced by interaction with DMPG. In addition, the binding of βLG to DMPG resulted in 4 and 6 nm blue shifts in the fluorescence λ_{max} at pH 6.8 and 4.6, respectively, indicating that the Trp residues remain shielded, presumably by the lipid bilayers.

Polarized ATR-FTIR was employed to determine the preferred orientations of βLG segments interacting with DMPG bilayer films on a surface. ATR-FTIR difference spectra are shown in Figure 8 for βLG associated with DMPG (250:1 DMPG:βLG ratio) at pH 4.6 and 6.8. The difference spectrum was obtained by subtracting the 0° polarized spectrum from the 90° polarized spectrum using a weight coefficient R_{iso} of 1.21 (see Materials and Methods) (*23*, *27*, *28*). In Figure 8, the $\gamma_w(CH_2)$ progression bands in the region of 1350−1180 cm^{-1}, arising from wagging motions of the lipid methylenes, appear as positive difference peaks, and the CH_2 scissoring band contributes a negative difference band at 1467 cm^{-1}, indicating that the lipid membranes have their hydrocarbon chains oriented preferentially along the normal to the plate. In the amide I region (1700−1600 cm^{-1}), the dichroic spectra for the DMPG-bound βLG at both pHs showed two positive bands at 1654 and 1637 cm^{-1}, which can be assigned to the helix and β-sheet components, respectively. For an α-helix, the amide I stretching vibration is oriented parallel to the helix axis, and therefore, the net positive peak at ∼1654 cm^{-1} indicates a preferred orientation of the helix axes perpendicular to the membrane surface at both pHs. Our method was tested by reproducing published results for melittin (*23*).

This interpretation has support from our oriented CD results (not shown). The CD spectrum of DMPG-bound βLG in solution exhibits two negative bands at 222 and 208 nm, a feature typical of helical structure. For βLG bound to a DMPG film, whose surface is perpendicular to the propagation of the circularly polarized light beams, a helical CD pattern is again observed; however, the 225 nm feature becomes more negative, while the 207 nm feature becomes less negative than that in solution. This is consistent with the helix having an orientational preference perpendicular to the membrane surface (*23*).

By contrast, for the β-sheet, the C═O stretching vibration is oriented perpendicular to the β-sheet strand direction, and therefore, the net positive feature observed for the β-sheet component of amide I′ at ∼1637 cm^{-1} indicates that the β-strands have a preferred orientation parallel to the membrane surface at both pHs. Due to the lack of resolution of the α-helix and β-sheet components and to the distinct possibility of there being several segments at different angles in this protein−vesicle complex, it is not sensible to analyze these spectra more quantitatively. Thus, we determine a propensity for the average orientation but do not determine an angle.

DISCUSSION

Interaction Force Governing the Association of βLG with Lipids. Interactions between proteins and lipids are different from chemical reactions in that typically no covalent bonds are involved. Instead, the association of a protein with a lipid membrane corresponds to a physical adsorption process through either electrostatic interaction, nonspecific interaction like hydrophobic interaction, or both (*35*). With regard to the governing forces between proteins and lipid membranes, some previous studies have concluded that the association of water-soluble proteins with lipids is primarily dependent on the overall electrostatic forces (*36*), while others implied that the hydrophobic interaction plays a main role (*37*) or that both electrostatic interaction and hydrophobic interaction are important (*38*, *39*). Clearly, this is not a settled area of research, and in particular, a general mechanism may not apply, which is apparent from the conflicts that prevail in the βLG literature (*16*, *17*, *40*).

Our CD and IR studies on systematically prepared βLG with lipid vesicles are consistent, both techniques showing

a clear β-to-α transition upon addition of anionic DMPG to βLG (Figures 1 and 2), accompanied by a substantial expansion of the tertiary structure (Figure 3). On the other hand, zwitterionic DMPC alone did not induce significant changes in the secondary or tertiary structure of βLG, consistent with the previous studies (*11*, *18*). Addition of DMPC to a preformed βLG−DMPG complex actually reduced the DMPG-induced α-helix content. Consistent with this, decreasing lipid charge (decreased DMPG fraction) greatly decreased the level of lipid-induced non-native α-helix in DMPG and DMPC mixtures with a fixed total lipid concentration and, hence, hydrophobic concentration (Figure 4B). These results show that dramatic changes in βLG secondary structure can be induced only by negatively charged lipids. Zwitterionic lipids alone cannot induce the conformational change at least under our experimental conditions, nor can they further increase the level of preformed DMPG-induced α-helix. Clearly, our results demonstrate that whereas the electrostatic interaction plays a major role in the lipid-induced non-native α-helix, the hydrophobic interaction plays a minor role. Extension of lipid-induced non-native helical structure and maintenance of the βLG structure in the lipid state may be dependent on the hydrophobic nature of the lipid bilayer since the salt alone cannot induce any induction of α-helix (see below).

Our pH study shows that anionic lipids can induce non-native α-helix for βLG at both acidic and basic pH (Figure 4A). When the pH is above the βLG isoelectric point of 5.5, the formation of α-helix appears to be a simple transition at the expense of the β-sheet fraction (Figure 1B). If the pH is lowered to 4.6, the fraction of DMPG-induced non-native α-helix can be increased further at the expense of both β-sheet and unordered fractions (∼36% at pH 6.8 and ∼56% at pH 4.6; Figure 1C). Such a behavior can be ascribed to the increase in positive charge at lower pH, further confirming the electrostatic driving force between βLG and the DMPG vesicles. Bergers (*36*) pointed out that significant adsorption of the proteins to negatively charged liposomes was found at only pH values where there was a net charge of +3 or more. This situation would obviously apply for βLG at pH 4.6, where the charge of βLG is approximately +8 or more. However, it immediately poses the question of how βLG can interact with negatively charged DMPG at pH 6.8 where the protein is negatively charged (net charge of approximately −10). Inspection of the three-dimensional structure of βLG shows that βLG has an inhomogeneous charge distribution (*34*). As a result, a region rich in positively charged residues on the βLG surface could preferentially come into contact with the negatively charged bilayer surface. That interaction could lead to a destabilization of the β-barrel or calyx-shell structure, relax the tertiary structure to allow insertion of segments into the bilayer, and thereby promote formation of an added helical component.

Ionic strength has always been employed in investigating how important the electrostatic interaction is in the association of proteins with lipids. Generally, screening of the charge of both the protein and lipids by adding salt results in reduction of the electrostatic interaction impact. In this study, binding of βLG to DMPG at pH 6.8 can be reversed to a great extent by increasing the NaCl concentration, whereas at pH 4.6, the βLG−DMPG complex shows resistance to dissociation by NaCl (Figure 5). This might be explained by the stronger interaction at lower pH, due to the higher positive charge accompanying protonation of βLG, resulting in more penetration of βLG into the lipid bilayers at lower pH. It is worth noting that at both pHs the βLG−DMPG complex cannot be completely dissociated by salt addition, further supporting the model in which portions of βLG are incorporated within the lipid bilayers.

Taken together, our results show that the binding of βLG to lipid membranes is primarily dependent on the overall electrostatic attraction between the lipid surface and protein-associated charges. The intermolecular electrostatic interactions may weaken the intramolecular forces that stabilize the native structure and eventually induce a significant perturbation in the βLG conformation. Since salt alone does not induce a change in the βLG structure, the hydrophobic aspect of the lipid indeed must play a role in the conformational transition, but these data do not speak to it directly. Our results for βLG−vesicle interaction are in good agreement with the previous LB trough studies of lipid monolayers at the air−water interface (*17*). An initially electrostatic interaction between polar groups is followed by hydrophobic interaction, which is enhanced through conformational changes that expose hydrophobic groups of βLG. However, our CD study does not support previous CD studies of films, in which no significant conformational change was observed on interaction with a neutral and partially negatively charged film (*16*). Given the concentration dependence of the interaction, it seems that the interaction could be surface-driven and becomes saturated, i.e., independent of an increase in DMPG concentration, when enough vesicles are available to bind all proteins. This could be consistent with the concentration dependence found which shows a maximal level of helix induced at 0.5 mM DMPG for far-UV CD experiments (0.01 mM protein), but for IR experiments (0.05 mM protein), a higher concentration of DMPG (∼10 mM) is required.

In DMPG, the structure of βLG in the α-state and the evolution of secondary structure are not the same as those induced by alcohols and ionic surfactants. TFE and other alcohols do have the potential of inducing formation of fractions of non-native α-helices (∼80%) larger than those which ionic surfactants or lipids can produce. Yet to induce the same level of non-native α-helical structure in βLG that is found with lipids, higher concentrations of alcohols would be required. More importantly, the TFE-induced α-state is unstable and readily converts to β-structure (*13*, *41*), whereas the lipid-induced α-dominant structure is stable in our hands. In addition, the βLG−DMPG complex cannot completely dissociate to the thermally unfolded state of βLG (Figure 6), presumably due to the partial insertion of the protein into the lipid bilayer.

Another milk protein, α-lactalbumin (αLA), also has a well-studied interaction with model membranes (*19*, *42*−*44*). It was found that formation of a flexible structural intermediate of αLA in solution is a prerequisite for its association with membranes (*43*). Native αLA does not bind to membranes, but binding can occur at pHs below and above its isoelectric point only if the protein is partially unfolded (*42*, *43*). The αLA protein is reversibly released from the membrane when the pH is increased. Obviously, this is not the case for the interaction of βLG with membranes since the native state βLG can bind to the membrane even above

its isoelectric point (Figure 1B). Previous work has largely shown that αLA as a molten globule-like state can bind to membranes (*19*, *42*, *43*); by contrast, βLG exhibits a clear β-to-α transition and also loses tertiary structure upon binding to membranes.

Insertion and Orientation of βLG to Lipid Bilayers. Fluorescence quenching can provide useful information about the solvent exposure or accessibility of tryptophan residues in proteins or proteins associated with lipid vesicles. When a protein inserts into lipid bilayers, tryptophan residues in proteins can be shielded by the hydrophobic interior, which could be accompanied by a blue shift in the fluorescence emission maximum (λ_{max}) and reduced quenching accessibility, as compared to the native state. βLG has two Trp residues that are differently exposed to the water solvent in the monomeric native state. From the crystal structure, Trp-19, facing the hydrophobic pocket, should be essentially inaccessible to the solvent, whereas Trp-61, at the end of one β-strand and close to the cystine 160−cystine 66 disulfide bond, is relatively exposed (*34*). By genetically modifying Trp-19 to alanine, Cho et al. found that the βLG fluorescence can be mainly attributed to Trp-19 residues while Trp-61 provides only a minor contribution, quenched by the nearby disulfide (*33*). Upon binding to lipids, the βLG tertiary structure expanded, and Trp-61 gained the possibility of moving away from its nearby quencher, as suggested by the increase in the fluorescence intensity (Figure 3A). Due to the partial insertion of the protein into the lipid bilayer, there is a blue shift in λ_{max} of 4 and 6 nm at pH 6.8 and 4.6, respectively, in contrast to a red shift that would have been expected if Trp had become exposed to solvent in an unfolded state. This indicates that the Trp residues in the DMPG-bound state remain in an environment roughly as nonpolar as that of the native state; i.e., the presence of vesicles partially shields the fluorophores from the aqueous solvent even though the tertiary structure is lost, which would be consistent with insertion of Trp-containing segments (at least one) into the bilayer.

Stern−Volmer analysis of the acrylamide-induced fluorescence quenching experiment (Figure 7), in which the Stern−Volmer quenching constant changes by only 10−20% after addition of DMPG to βLG at pH 4.6 and 6.8, indicates that the accessibility of the tryptophans to the neutral acrylamide quencher in membrane-bound βLG at both pHs is almost the same as in the native state. Since βLG becomes less compact once bound to DMPG (as demonstrated by the loss of near-UV CD and the increase in fluorescence intensity, as seen in Figure 3), the tryptophans should have been more easily quenched by added acrylamide, if the lipid did not shield them. Given that the tertiary structure is lost on DMPG binding at this concentration, the similarity in quenching could imply partial penetration of βLG into the lipid membrane. Compared with that of the membrane-bound βLG at pH 6.8, the larger blue shift as well as a smaller quenching constant might imply more insertion at pH 4.6, but the changes are small. This is consistent with the previous monolayer study (*17*) in which it was thought that portions of the protein were intercalated in the lipid monolayer. Presumably, a conformational change in the water-soluble protein, stimulated by electrostatic interaction with charged lipid headgroups, exposes hydrophobic patches from the protein that could trigger partial insertion into the membrane.

On the basis of these observations, we hypothesize that βLG is partially incorporated into anionic lipid vesicles and that at pHs above and below its isoelectric point the secondary structure of membrane-bound βLG is comprised of predominantly non-native α-helix as well as some residual native β-sheet. Our polarized ATR-FTIR results demonstrate that the α-helical axes are oriented orthogonally to the lipid CH_2 wag modes and thus are preferentially perpendicular to the membrane surface, while the residual β-sheet axes are more parallel to the membrane surface (Figure 8). This analysis is in good agreement with oriented CD results (data not shown), where a decrease in ellipticity at 207 nm and an increase at 225 nm confirm that the helical segments are oriented parallel to the light propagation direction (*23*, *24*). The parallels of ATR, oriented CD, and solution phase vesicle-induced conformational change for βLG confirm that the phenomenon is induced by the lipid bilayer and controlled by the charge interaction.

CONCLUSIONS

Negatively charged phospholipids, like alcohols and surfactants, can induce a high degree of non-native α-helical structure in βLG. However, the mechanism of the interaction between the protein and lipids, the structure of the lipid-induced α-helical state, the evolution of the lipid-induced β-to-α transition, and the stability of the lipid-induced complex are different from those between the protein and alcohols or surfactants. The adsorption of βLG onto lipid surface is governed by intermolecular electrostatic interaction between βLG and lipid membranes and thereby may weaken the intramolecular forces that stabilize the native structure to cause βLG conformational transition on the membrane surface. Once the tightly packed βLG is disturbed, hydrophobic residues become exposed and readily available for the insertion, which further extends non-native α-helical structure. In the lipid-bound α-helical state, α-helix and β-sheet strands are perpendicular and parallel, respectively, to the membrane surface. This study may help explain one possible biological function of βLG, as an intracellular transporter of fatty acids, since the transportation of fatty acids is enabled by the interaction between the fatty acid-binding proteins and lipid vesicles via either a diffusion-controlled mechanism or a direct collision of the proteins with the membrane (*45*).

ACKNOWLEDGMENT

We thank Dr. Qi Xu and Rong Huang for help with preliminary experiments and suggestions for data analysis.

REFERENCES

1. Sawyer, L., and Kontopidis, G. (2000) The core lipocalin, bovine β-lactoglobulin, *Biochim. Biophys. Acta 1482*, 136−148.
2. Qin, B. Y., Creamer, L. K., Baker, E. N., and Jameson, G. B. (1998) 12-Bromododecanoic acid binds inside the calyx of bovine β-lactoglobulin, *FEBS Lett. 438*, 272−278.
3. Ragona, L., Fogolari, F., Zetta, L., Perez, D. M., Puyol, P., De Kruif, K., Lohr, F., Ruterjans, H., and Molinari, H. (2000) Bovine β-lactoglobulin: Interaction studies with palmitic acid, *Protein Sci. 9*, 1347−1356.
4. Kobayashi, T., Ikeguchi, M., and Sugai, S. (2000) Molten globule structure of equine β-lactoglobulin probed by hydrogen exchange, *J. Mol. Biol. 299*, 757−770.
5. Kuwajima, K., Yamaya, H., Miwa, S., Sugai, S., and Nagamura, T. (1987) Rapid formation of secondary structure framework in

protein folding studied by stopped-flow circular dichroism, *FEBS Lett. 221*, 115−118.
6. Kuwajima, K., Yamaya, H., and Sugai, S. (1996) The burst-phase intermediate in the refolding of β-lactoglobulin spectroscopy, *J. Mol. Biol. 264*, 806−822.
7. Shiraki, K., Nishikawa, K., and Goto, Y. (1995) Trifluoroethanol-induced stabilization of the α-helical structure of β-lactoglobulin: Implication for non-hierachical protein folding, *J. Mol. Biol. 245*, 180−194.
8. Forge, V., Hoshino, M., Kuwata, K., Arai, M., Kuwajima, K., Batt, C. A., and Goto, Y. (2000) Is folding of β-lactoglobulin non-hierarchic? Intermediate with native-like β-sheet and non-native α-helix, *J. Mol. Biol. 296*, 1039−1051.
9. Mendieta, J., Folqué, H., and Tauler, R. (1999) Two-phase induction of the nonnative α-helical form of β-lactoglobulin in the presence of trifluoroethanol, *Biophys. J. 76*, 451−457.
10. Creamer, L. K. (1995) Effect of sodium dodecyl sulfate and palmitic acid on the equilibrium unfolding of bovine β-lactoglobulin, *Biochemistry 34*, 7170−7176.
11. Lefevre, T., and Subirade, M. (2000) Interaction of β-lactoglobulin with phospholipid bilayers: A molecular level elucidation as revealed by infrared spectroscopy, *Int. J. Biol. Macromol. 28*, 59−67.
12. Hirota, N., Mizuno, K., and Goto, Y. (1997) Cooperative α-helix formation of β-lactoglobulin and melittin induced by hexafluoroisopropanol, *Protein Sci. 6*, 416−421.
13. Dong, A., Matsuura, J., Manning, M. C., and Carpenter, J. F. (1998) Intermolecular β-sheet results from trifluoroethanol-induced nonnative α-helical structure in β-sheet predominant proteins: Infrared and circular dichroism spectroscopic study, *Arch. Biochem. Biophys. 355*, 275−281.
14. Jones, M. N. (1992) Surfactant interactions with biomembranes and proteins, *Chem. Soc. Rev. 34*, 127−136.
15. Cornell, D. G., and Carroll, R. J. (1985) Miscibility in lipid−protein monolayers, *J. Colloid Interface Sci. 108*, 226−233.
16. Cornell, D. G., and Patterson, D. L. (1989) Interaction of phospholipids in monolayers with β-lactoglobulin adsorbed from solution, *J. Agric. Food Chem. 37*, 1455−1459.
17. Bos, M. A., and Nylander, T. (1996) Interaction between β-lactoglobulin and phospholipids at the air/water interface, *Langmuir 12*, 2791−2797.
18. Lefevre, T., and Subirade, M. (2001) Conformational rearrangement of β-lactoglobulin upon interaction with an anionic membrane, *Biochim. Biophys. Acta 1549*, 37−50.
19. Agasøster, A. V., Halskau, Ø., Fuglebakk, E., Frøystein, N., Muga, A., Holmsen, H., and Martínez, A. (2003) The interaction of peripheral proteins and membranes studied with α-lactalbumin and phospholipid bilayers of various compositions, *J. Biol. Chem. 278*, 21790−21797.
20. Schneider, M. F., Marsh, D., Jahn, W., Kloesgen, B., and Heimburg, T. (1999) Network formation of lipid membranes: Triggering structural transitions by chain melting, *Proc. Natl. Acad. Sci. U.S.A. 96*, 14312−14317.
21. Sreerama, N., and Woody, R. W. (2000) Estimation of protein secondary structure from circular dichroism spectra: Comparison of CONTIN, SELCON, and CDSSTR methods with an expanded reference set, *Anal. Biochem. 287*, 252−260.
22. Mao, D., and Wallace, B. A. (1984) Differential light scattering and absorption flattening optical effects are minimal in the circular dichroism spectra of small unilamellar vesicles, *Biochemistry 23*, 2667−2673.
23. de Jongh, H. H. J., Goormaghtigh, E., and Killian, J. A. (1994) Analysis of circular dichroism spectra of oriented protein−lipid complexes: Toward a general application, *Biochemistry 33*, 14521−14528.
24. Wu, Y., Huang, H. W., and Olah, G. A. (1990) Method of oriented circular dichroism, *Biophys. J. 57*, 797−806.
25. Xu, Q., and Keiderling, T. A. (2004) Effect of sodium dodecyl sulfate on folding and thermal stability of acid-denatured cytochrome *c*: A spectroscopic approach, *Protein Sci. 13*, 2949−2959.
26. Xu, Q., and Keiderling, T. A. (2005) Trifluoroethanol-induced unfolding of concanavalin A: Equilibrium and time-resolved optical spectroscopic studies, *Biochemistry 44*, 7976−7987.
27. Goormaghtigh, E., Raussens, V., and Ruysschaert, J. M. (1999) Attenuated total reflection infrared spectroscopy of proteins and lipids in biological membranes, *Biochim. Biophys. Acta 1422*, 105−185.
28. Tatulian, S. A. (2003) Attenuated total reflection Fourier transform infrared spectroscopy: A method of choice for studying membrane proteins and lipids, *Biochemistry 42*, 11898−11907.
29. Lakowicz, J. R. (1983) *Principles of fluorescence spectrosopy*, Plenum Press, New York.
30. Pancoska, P., Bitto, E., Janota, V., Urbanova, M., Gupta, V. P., and Keiderling, T. A. (1995) Comparison of and limits of accuracy for statistical analyses of vibrational and electronic circular dichroism spectra in terms of correlations to and predictions of protein secondary structure, *Protein Sci. 4*, 1384−1401.
31. Andrade, S. M., Carvalho, T. I., Viseu, M. I., and Costa, S. M. B. (2004) Conformational changes of β-lactoglobulin in sodium bis-(2-ethylhexyl) sulfosuccinate reverse micelles: A fluorescence and CD study, *Eur. J. Biochem. 271*, 734−744.
32. Berova, N., Nakanishi, K., and Woody, R. W. (2000) *Circular Dichroism*, Wiley-VCH, New York.
33. Cho, Y., Batt, C. A., and Sawyer, L. (1994) Probing the retinol-binding site of bovine β-lactoglobulin, *J. Biol. Chem. 269*, 11102−11107.
34. Fogolari, F., Ragona, L., Licciardi, S., Romagnoli, S., Michelutti, R., Ugolini, R., and Molinari, H. (2000) Electrostatic properties of bovine β-lactoglobulin, *Proteins: Struct., Funct., Genet. 39*, 317−330.
35. Bañuelos, S., and Muga, A. (1996) Structural requirements for the association of native and partially folded conformations of α-lactalbumin with model membranes, *Biochemistry 35*, 3892−3898.
36. Bergers, J. J., Vingerhoeds, M. H., van Bloois, L., Herron, J. N., Janssen, L. H. M., Fischer, M. J. E., and Crommelin, D. J. A. (1993) The role of protein charge in protein−lipid interactions. pH-dependent changes of the electrophoretic mobility of liposomes through adsorption of water-soluble, globular proteins, *Biochemistry 32*, 4641−4649.
37. Cevc, G., Strohmaier, L., Berkholz, J., and Blume, G. (1990) Molecular mechanism of protein interactions with the lipid bilayer membrane, *Stud. Biophys. 138*, 57−70.
38. Leenhouts, J. M., van den Wijngaard, P. W. J., de Kroon, A. I. P. M., and de Kruijff, B. (1995) Anionic phospholipids can mediate membrane insertion of the anionic part of a bound peptide, *FEBS Lett. 370*, 189−192.
39. Snel, M. M., de Kroon, A. I. P. M., and Marsh, D. (1995) Mitochondrial presequence inserts differently into membranes containing cardiolipin and phosphatidylglycerol, *Biochemistry 34*, 3605−3613.
40. Brown, E. M., Carroll, R. J., Pfeffer, P. E., and Sampugna, J. (1983) Complex formation in sonicated mixtures of β-lactoglobulin and phosphatidylcholine, *Lipids 18*, 111−118.
41. Barteri, M., Gaudiano, M. C., Mei, G., and Rosato, N. (1998) New stable folding of β-lactoglobulin induced by 2-propanol, *Biochim. Biophys. Acta 1383*, 317−326.
42. Banuelos, S., and Muga, A. (1995) Binding of molten globule-like conformations to lipid bilayers. Structure of native and partially folded α-lactalbumin bound to model membranes, *J. Biol. Chem. 270*, 29910−29915.
43. Banuelos, S., and Muga, A. (1996) Structural requirements for the association of native and partially folded conformations of α-lactalbumin with model membranes, *Biochemistry 35*, 3892−3898.
44. Rodland, I., Halskau, O., Martinez, A., and Holmsen, H. (2005) α-Lactalbumin binding and membrane integrity: Effect of charge and degree of unsaturation of glycerophospholipids, *Bichim. Biophys. Acta 1717*, 11−20.
45. Nolan, V., Perduca, M., Monaco, H. L., Maggio, B., and Montich, G. G. (2003) Interactions of chicken liver basic fatty acid-binding protein with lipid membranes, *Biochim. Biophys. Acta 1611*, 98−106.

BI0602967